Advanced Coupling Matrix Synthesis Techniques for Microwave Filters

Richard J. Cameron, *Fellow, IEEE*

Abstract—**A general method is presented for the synthesis of the folded-configuration coupling matrix for Chebyshev or other filtering functions of the most general kind, including the fully canonical case, i.e., N prescribed finite-position transmission zeros in an Nth-degree network. The method is based on the "$N + 2$" transversal network coupling matrix, which is able to accommodate multiple input/output couplings, as well as the direct source–load coupling needed for the fully canonical cases. Firstly, the direct method for building up the coupling matrix for the transversal network is described. A simple nonoptimization process is then outlined for the conversion of the transversal matrix to the equivalent "$N + 2$" folded-configuration coupling matrix. The folded matrix may be used directly to realize microwave bandpass filters in a variety of technologies, but some of these could require awkward-to-realize cross-couplings. This paper concludes with a description of two simple procedures for transforming the transversal and folded matrices into two novel network configurations, which enable the realization of advanced microwave bandpass filters without the need for complex inter-resonator coupling elements.**

Index Terms—**Asymmetric filtering functions, Chebyshev characteristics, circuit synthesis methods, coupling matrix, microwave filters, transversal network.**

I. Introduction

In [1], a recursive method for deriving the transfer and reflection polynomials for Chebyshev filtering functions with prescribed finite-position transmission zeros (TZs) was presented. This was followed by the synthesis methods for the corresponding "$N \times N$" coupling matrix, ready for the realization of a microwave filter with resonators arranged as a folded cross-coupled array. It was mentioned in [1] that, although the polynomial synthesis procedure was capable of generating N TZs for an Nth-degree network (i.e., fully canonical), that a maximum of only $N - 2$ finite-position zeros could be realized by the $N \times N$ coupling matrix. This precluded some useful filtering characteristics, including those that require multiple input/output couplings, which have been finding applications recently [3].

In this paper, a method is presented for the synthesis of the fully-canonical or "$N+2$" folded coupling matrix, which overcomes some of the shortcomings of the conventional $N \times N$ coupling matrix. The $N+2$ or "extended" coupling matrix has an extra pair of rows top and bottom and an extra pair of columns left and right surrounding the "core" $N \times N$ coupling matrix, which carry the input and output couplings from the source and load terminations to resonator nodes in the core matrix.

Manuscript received November 2, 2001.
The author is with COM Dev International Ltd., Aylesbury HP22-5SX, U.K.
Digital Object Identifier 10.1109/TMTT.2002.806937

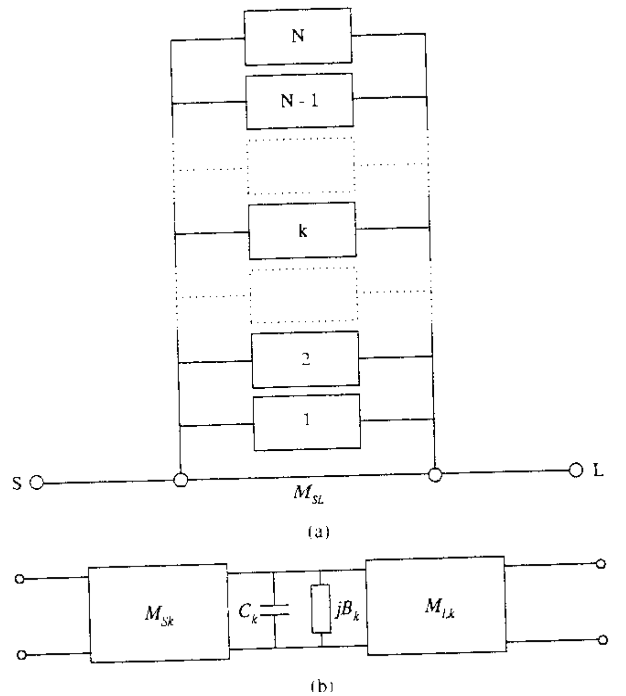

Fig. 1. Canonical transversal array. (a) N—resonator transversal array including direct source–load coupling M_{SL}. (b) Equivalent circuit of the kth "low-pass resonator" in the transversal array.

The $N+2$ matrix has the following advantages, as compared with the conventional coupling matrix.

- Multiple input/output couplings may be accommodated, i.e., couplings may be made directly from the source and/or to the load to internal resonators, in addition to the main input/output couplings to the first and last resonator in the filter circuit.
- Fully canonical filtering functions (i.e., Nth-degree characteristics with N finite-position TZs) may be synthesized.
- During certain synthesis procedures that employ a sequence of similarity transforms (rotations), it is sometimes convenient to temporarily "park" couplings in the outer rows or columns, whilst other rotations are carried out elsewhere in the matrix.

The paper begins by detailing the procedure for synthesizing the $N+2$ coupling matrix from the transversal array circuit representation of the filtering function (see Figs. 1(a) and 2), which follows on from the methods originally established in [4]–[7] and later extended in [1]. The new method is actually simpler to derive than those used to synthesize the $N \times N$ coupling matrix, not requiring the Gram–Schmidt orthonormalization stage. The

	S	1	2	3	..	k	..	$N\text{-}1$	N	L
S		M_{S1}	M_{S2}	M_{S3}	..	M_{Sk}	..	$M_{S,N-1}$	M_{SN}	M_{SL}
1	M_{1S}	M_{11}								M_{1L}
2	M_{2S}		M_{22}							M_{2L}
3	M_{3S}			M_{33}						M_{3L}
:	:				$\ddots$					:
k	M_{kS}					M_{kk}				M_{kL}
:	:						$\ddots$			:
$N\text{-}1$	$M_{N-1,S}$							$M_{N-1,N-1}$		$M_{N-1,L}$
N	M_{NS}								M_{NN}	M_{NL}
L	M_{LS}	M_{L1}	M_{L2}	M_{L3}	..	M_{Lk}	..	$M_{L,N-1}$	M_{LN}	

Fig. 2. $N + 2$ fully canonical coupling matrix [M] for the transversal array. The "core" $N \times N$ matrix is indicated within the double lines. The matrix is symmetric about the principal diagonal, i.e., $M_{ij} = M_{ji}$.

reduction of the transversal coupling matrix to the $N+2$ folded cross-coupled array coupling matrix is then outlined, following much the same procedure as in [1]. A demonstration of the use of the techniques to synthesize the coupling matrix for a fully canonical filtering function is included.

Finally, the direct synthesis of two novel filter configurations are presented; one starting with the transversal coupling matrix and the second based on the folded coupling matrix. Both are applicable to the design of microwave bandpass filters in a variety of technologies, but the second, in particular, has some important implementation advantages that should considerably ease the design and production of high performance filters for space or terrestrial communications systems.

II. Synthesis of the "$N + 2$" Transversal Coupling Matrix

The approach that will be employed to synthesize the $N + 2$ transversal coupling matrix will be to construct the two-port short-circuit admittance parameter matrix $[Y_N]$ for the overall network in two ways; the first from the coefficients of the rational polynomials of the transfer and reflection scattering parameters $S_{21}(s)$ and $S_{11}(s)$, which represent the characteristics of the filter to be realized, and the second from the circuit elements of the transversal array network. By equating the $[Y_N]$ matrices as derived by these two methods, the elements of the coupling matrix associated with the transversal array network may be related to the coefficients of the $S_{21}(s)$ and $S_{11}(s)$ polynomials.

A. Synthesis of Admittance Function $[Y_N]$ From the Transfer and Reflection Polynomials

The transfer and reflection polynomials that are generated in [1] for the general Chebyshev filtering function are in the form

$$S_{21}(s) = \frac{P(s)}{\varepsilon E(s)} \quad S_{11}(s) = \frac{F(s)}{\varepsilon_R E(s)} \tag{1}$$

where $\varepsilon = (1/\sqrt{10^{RL/10} - 1}) \cdot (P(s)/F(s))|_{s=j}$, RL is the prescribed return loss in decibels, and it is assumed that the polynomials $E(s)$, $F(s)$, and $P(s)$ have been normalized to their respective highest degree coefficients. Both $E(s)$ and $F(s)$ are Nth-degree polynomials, N is the degree of the filtering function, whilst $P(s)$, which contains the finite-position prescribed TZs, is of degree n_{fz}, where n_{fz} is the number of finite-position TZs that have been prescribed. For a realizable network, n_{fz} must be $\leq N$.

ε_R is unity for all cases except for fully canonical filtering functions, where all the TZs are prescribed at finite frequencies, i.e., $n_{fz} = N$. In this case, the value of $S_{21}(s)$ (in decibels) is finite at infinite frequency, and if the highest degree coefficient of the polynomials $E(s)$, $F(s)$, and $P(s)$ are each normalized to unity, ε_R will have a value slightly greater than unity as follows:

$$\varepsilon_R = \frac{\varepsilon}{\sqrt{\varepsilon^2 - 1}}. \tag{2}$$

It is also important to ensure that the transfer and reflection vectors are orthogonal in order to satisfy the unitary conditions for the scattering matrix [8]

$$\begin{aligned} S_{11} \cdot S_{11}^* + S_{21} \cdot S_{21}^* &= 1 \\ S_{22} \cdot S_{22}^* + S_{12} \cdot S_{12}^* &= 1 \\ S_{11} \cdot S_{12}^* + S_{21} \cdot S_{22}^* &= 0. \end{aligned} \tag{3}$$

From (3), it may be shown (see [2, p. 177]) that the phases ϕ, θ_1, and θ_2 of the vectors $S_{21}(s)$, $S_{11}(s)$, and $S_{22}(s)$, respectively, are related by the following:

$$\phi - \frac{\theta_1 + \theta_2}{2} = \Delta_\varphi = \frac{\pi}{2}(2k \pm 1) \tag{4}$$

where k is an integer.

Equation (4) shows that the difference Δ_φ between the phase of the S_{21} vector, and the average of the phases of the S_{11} and S_{22} vectors must be an odd multiple of $\pi/2$ rad. For this condition to be satisfied at any value of the frequency variable s, the n_{fz} TZs of $S_{21}(s)$ must be positioned symmetrically about the imaginary ($j\omega$) axis or upon the imaginary axis itself. Similarly, the pattern of the N zeros of $S_{22}(s)$ must either be coincident with those of $S_{11}(s)$ on the imaginary axis, or form mirror-image pairs about the imaginary axis with corresponding off-axis zeros of $S_{11}(s)$. In this way, the sum of the phases of the individual vectors that make up the overall phases of the vectors S_{21}, S_{11}, etc., will be multiples of $\pi/2$ rad.

Since $S_{21}(s)$, $S_{11}(s)$, and $S_{22}(s)$ share a common denominator polynomial $E(s)$, it is only necessary to consider their numerator polynomials as far as (4) is concerned. The multiples of $\pi/2$ rad referred to above therefore depend upon the number of finite-position transmit (Tx) zeros n_{fz} for the $S_{21}(s)$ numerator polynomial $P(s)$, and the degree N of the filtering function for the $S_{11}(s)$ and $S_{22}(s)$ numerator polynomials ($F(s)$ and $F^*(s)$, respectively). With this in mind, it follows that, for the left-hand side of (4) to produce an odd multiple of $\pi/2$ rad, the integer quantity $N - n_{fz}$ must itself be odd. Thus, to ensure orthogonality between the $F(s)$ and $P(s)$ vectors, i.e., Δ_ϕ is an odd multiple of $\pi/2$ rad, it is necessary to multiply the $P(s)$ polynomial by j whenever $N - n_{fz}$ is an even integer.

The numerator and denominator polynomials for the $y_{21}(s)$ and $y_{22}(s)$ elements of $[Y_N]$ may be built up directly from the transfer and reflection polynomials for $S_{21}(s)$ and $S_{11}(s)$ [1]. For a double-terminated network with source and load terminations of 1 Ω

$$y_{22}(s) = y_{22n}(s)/y_d(s) = n_1(s)/m_1(s)$$

and

$$y_{21}(s) = y_{21n}(s)/y_d(s) = \left(P(s)/\varepsilon\right)/m_1(s). \qquad \text{for } N \text{ even}$$
$$y_{22}(s) = y_{22n}(s)/y_d(s) = m_1(s)/n_1(s)$$

and

$$y_{21}(s) = y_{21n}(s)/y_d(s) = \left(P(s)/\varepsilon\right)/n_1(s). \qquad \text{for } N \text{ odd}$$

where

$$\begin{aligned} m_1(s) &= \mathrm{Re}(e_0+f_0)+j\mathrm{Im}(e_1+f_1)s+\mathrm{Re}(e_2+f_2)s^2+\cdots \\ n_1(s) &= j\mathrm{Im}(e_0+f_0)+\mathrm{Re}(e_1+f_1)s+j\mathrm{Im}(e_2+f_2)s^2+\cdots \end{aligned} \tag{5}$$

and e_i and f_i, $i = 0, 1, 2, 3, \ldots, N$ are the complex coefficients of $E(s)$ and $F(s)/\varepsilon_R$, respectively. The $y_{21}(s)$ and $y_{22}(s)$ polynomials for single-terminated networks may be found by a similar procedure [1].

Knowing the denominator and numerator polynomials for $y_{21}(s)$ and $y_{22}(s)$, their residues r_{21k} and r_{22k}, $k = 1, 2, \ldots, N$ may be found with partial fraction expansions, and the purely real eigenvalues λ_k of the network found by rooting the denominator polynomial $y_d(s)$ common to both $y_{21}(s)$ and $y_{22}(s)$, which has purely imaginary roots $= j\lambda_k$ (see [1, Appendix]). Expressing the residues in matrix form yields the following equation for the admittance matrix $[Y_N]$ for the overall network:

$$\begin{aligned} [Y_N] &= \begin{bmatrix} y_{11}(s) & y_{12}(s) \\ y_{21}(s) & y_{22}(s) \end{bmatrix} \\ &= \frac{1}{y_d(s)} \begin{bmatrix} y_{11n}(s) & y_{12n}(s) \\ y_{21n}(s) & y_{22n}(s) \end{bmatrix} \\ &= j\begin{bmatrix} 0 & K_0 \\ K_0 & 0 \end{bmatrix} + \sum_{k=1}^{N} \frac{1}{(s-j\lambda_k)} \cdot \begin{bmatrix} r_{11k} & r_{12k} \\ r_{21k} & r_{22k} \end{bmatrix} \end{aligned} \tag{6}$$

where the real constant $K_0 = 0$, except for the fully canonical case where the number of finite-position TZs n_{fz} in the filtering function is equal to the filter degree N. In this case, the degree of the numerator of $y_{21}(s)$ $(y_{21n}(s), = jP(s)/\varepsilon)$ is equal to its denominator $y_d(s)$, and K_0 has to be extracted from $y_{21}(s)$ $(=y_{12}(s))$ first to reduce the degree of its numerator polynomial $y_{21n}(s)$ by one before its residues r_{21k} may be found. Note that, in the fully canonical case, where the integer quantity $N - n_{fz} = 0$ is even, it is necessary to multiply $P(s)$ by j to ensure that the unitary conditions for the scattering matrix are satisfied.

Being independent of s, K_0 may be evaluated at $s = j\infty$ as follows:

$$jK_0 = \left.\frac{y_{21n}(s)}{y_d(s)}\right|_{s=j\infty} = \left.\frac{jP(s)/\varepsilon}{y_d(s)}\right|_{s=j\infty}. \tag{7}$$

The process for building up y_d [see (5)] results in its highest degree coefficient having a value of $1 + 1/\varepsilon_R$ and, since the highest degree coefficient of $P(s) = 1$, the value of K_0 may be found as follows:

$$K_0 = \frac{1}{\varepsilon} \cdot \frac{1}{(1+1/\varepsilon_R)} = \frac{\varepsilon_R}{\varepsilon} \cdot \frac{1}{(\varepsilon_R+1)}. \tag{8}$$

The new numerator polynomial $y'_{21n}(s)$ may now be determined as follows:

$$y'_{21n}(s) = y_{21n}(s) - jK_0 y_d(s) \tag{9}$$

which will be of degree $N-1$, and the residues r_{21k} of $y'_{21}(s) = y'_{21n}(s)/y_d(s)$ may now be found as normal.

B. *Synthesis of Admittance Function $[Y_N]$—Circuit Approach*

The two-port short-circuit admittance parameter matrix $[Y_N]$ for the overall network may also be synthesized directly from the fully canonical transversal network, the general form of which is shown in Fig. 1(a). It comprises a series of N individual first-degree low-pass sections, connected in parallel between the source and load terminations, but not to each other. The direct source–load coupling inverter M_{SL} is included to allow fully canonical transfer functions to be realized, according to the "minimum path" rule, i.e., $n_{fz\,\max}$, the maximum number of finite position TZs that may be realized by the network $= N - n_{\min}$, where $n_{\min}$ is the number of resonators in the shortest route through the network between the source and load terminations. In fully canonical networks $n_{\min} = 0$ and, thus, $n_{fz\,\max} = N$, the degree of the network.

Each of the N low-pass sections comprises one parallel-connected capacitor C_k and one frequency invariant susceptance B_k, connected through admittance inverters of characteristic admittances M_{Sk} and M_{Lk} to the source and load terminations, respectively. The circuit of the kth low-pass section is shown in Fig. 1(b).

Fully Canonical Filtering Functions

The direct source–load inverter M_{SL} in Fig. 1(a) is zero except for fully canonical filtering functions, where the number of finite-position zeros equals the degree of the filter. At infinite frequency ($s = \pm j\infty$), all the capacitors C_k become parallel short circuits, which appear as open circuits at the source–load ports through the inverters M_{Sk} and M_{Lk}. Thus, the only path between source and load is via the frequency-invariant admittance inverter M_{SL}.

If the load impedance is 1 Ω, the driving point admittance $Y_{11\infty}$ looking in at the input port will be (Fig. 3)

$$Y_{11\infty} = M_{SL}^2.$$

Therefore, the input reflection coefficient $S_{11}(s)$ at $s = j\infty$ is

$$S_{11}(s)|_{s=j\infty} \equiv |S_{11\infty}| = \frac{(1-Y_{11\infty})}{(1+Y_{11\infty})}. \tag{10}$$

Substituting for $|S_{11\infty}|$ in the conservation of energy equation using (10)

$$\begin{aligned} |S_{21\infty}| &= \sqrt{1-|S_{11\infty}|^2} \\ &= \frac{2\sqrt{Y_{11\infty}}}{(1+Y_{11\infty})} = \frac{2M_{SL}}{\left(1+M_{SL}^2\right)}. \end{aligned}$$

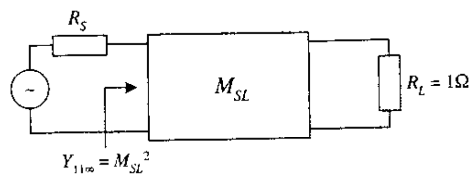

Fig. 3. Equivalent circuit of transversal array at $s = \pm j\infty$.

Solving for $M_{\rm SL}$

$$M_{\rm SL} = \frac{1 \pm \sqrt{1 - |S_{21\infty}|^2}}{|S_{21\infty}|} = \frac{1 \pm |S_{11\infty}|}{|S_{21\infty}|}.$$

At infinite frequency $|S_{21}(j\infty)| = (P(j\infty)/\varepsilon)/E(j\infty) = 1/\varepsilon$ because, for a fully canonical filtering function, P and E will both be Nth-degree polynomials with their highest degree coefficients normalized to unity. Similarly, $|S_{11}(j\infty)| = (F(j\infty)/\varepsilon_R)/E(j\infty) = 1/\varepsilon_R$. Therefore,

$$M_{\rm SL} = \frac{\varepsilon(\varepsilon_R \pm 1)}{\varepsilon_R}.$$

Since ε_R is slightly greater than unity for a fully canonical network, choosing the negative sign will give a relatively small value for $M_{\rm SL}$

$$M_{\rm SL} = \frac{\varepsilon(\varepsilon_R - 1)}{\varepsilon_R} \tag{11}$$

and correctly gives $M_{\rm SL} = 0$ for noncanonical filters, where $\varepsilon_R = 1$. It can be shown that the positive sign will give a second solution $M'_{\rm SL} = 1/M_{\rm SL}$, but since this will be a large number, it is never used in practice [8].

Synthesis of Two-Port Admittance Matrix $[Y_N]$

Cascading the elements in Fig. 1(b) gives an $ABCD$ transfer matrix for the kth "low-pass resonator" as follows:

$$[ABCD]_k = -\begin{bmatrix} \dfrac{M_{Lk}}{M_{Sk}} & \dfrac{(sC_k + jB_k)}{M_{Sk}M_{Lk}} \\ 0 & \dfrac{M_{Sk}}{M_{Lk}} \end{bmatrix} \tag{12}$$

which may then be directly converted into the equivalent short-circuit y-parameter matrix

$$\begin{aligned}[y_k] &= \begin{bmatrix} y_{11k}(s) & y_{12k}(s) \\ y_{21k}(s) & y_{22k}(s) \end{bmatrix} \\ &= \frac{M_{Sk}M_{Lk}}{(sC_k + jB_k)} \cdot \begin{bmatrix} \dfrac{M_{Sk}}{M_{Lk}} & 1 \\ 1 & \dfrac{M_{Lk}}{M_{Sk}} \end{bmatrix} \\ &= \frac{1}{(sC_k + jB_k)} \cdot \begin{bmatrix} M_{Sk}^2 & M_{Sk}M_{Lk} \\ M_{Sk}M_{Lk} & M_{Lk}^2 \end{bmatrix}. \end{aligned} \tag{13}$$

The two-port short-circuit admittance matrix $[Y_N]$ for the parallel-connected transverse array is the sum of the y-parameter matrices for the N individual sections, plus the y-parameter matrix $[y_{\rm SL}]$ for the direct source–load coupling inverter $M_{\rm SL}$

$$\begin{aligned}[Y_N] &= \begin{bmatrix} y_{11}(s) & y_{12}(s) \\ y_{21}(s) & y_{22}(s) \end{bmatrix} \\ &= [y_{\rm SL}] + \sum_{k=1}^{N} \begin{bmatrix} y_{11k}(s) & y_{12k}(s) \\ y_{21k}(s) & y_{22k}(s) \end{bmatrix} \\ &= j\begin{bmatrix} 0 & M_{\rm SL} \\ M_{\rm SL} & 0 \end{bmatrix} + \sum_{k=1}^{N} \frac{1}{(sC_k + jB_k)} \\ &\quad \cdot \begin{bmatrix} M_{Sk}^2 & M_{Sk}M_{Lk} \\ M_{Sk}M_{Lk} & M_{Lk}^2 \end{bmatrix}. \end{aligned} \tag{14}$$

C. Synthesis of the $N+2$ Transversal Matrix

Now the two expressions for $[Y_N]$, the first in terms of the residues of the transfer function (6), and the second in terms of the circuit elements of the transversal array (14), may be equated. It may be seen immediately that $M_{\rm SL} = K_0$, and for the "21" and "22" elements in the matrices in the right-hand sides of (6) and (14)

$$\frac{r_{21k}}{(s - j\lambda_k)} = \frac{M_{Sk}M_{Lk}}{(sC_k + jB_k)} \tag{15a}$$

$$\frac{r_{22k}}{(s - j\lambda_k)} = \frac{M_{Lk}^2}{(sC_k + jB_k)}. \tag{15b}$$

The residues r_{21k} and r_{22k} and the eigenvalues λ_k have already been derived from the S_{21} and S_{22} polynomials of the desired filtering function [see (5)] and, thus, by equating the real and imaginary parts in (15a) and (15b), it becomes possible to relate them directly to the circuit parameters

$$C_k = 1 \text{ and } B_k(\equiv M_{kk}) = -\lambda_k$$
$$M_{Lk}^2 = r_{22k} \text{ and } M_{Sk}M_{Lk} = r_{21k}$$

$\therefore$

$$M_{Lk} = \sqrt{r_{22k}} = T_{Nk}$$

and

$$M_{Sk} = r_{21k} / \sqrt{r_{22k}} = T_{1k}, \qquad k = 1, 2, \ldots, N. \tag{16}$$

It may be recognized at this stage that M_{Sk} and M_{Lk} constitute the unscaled row vectors T_{1k} and T_{Nk} of the orthogonal matrix $[\mathbf{T}]$, as defined in [1, Appendix].

Since the capacitors C_k of the parallel networks are all unity, and the frequency-invariant susceptances B_k $(=-\lambda_k$, representing the self couplings $M_{11} \rightarrow M_{NN})$, the input couplings M_{Sk}, the output couplings M_{Lk}, and the direct source–load coupling $M_{\rm SL}$ are all now known, the reciprocal $N + 2$ transversal coupling matrix $[\mathbf{M}]$ representing the network in Fig. 1(a) may now be constructed. M_{Sk} $(=T_{1k})$ are the N input couplings and occupy the first row and column of the matrix from positions 1 to N (see Fig. 2). Similarly, M_{Lk} $(=T_{Nk})$ are the N output couplings and they occupy the last row and column of $[\mathbf{M}]$ from positions 1 to N. All other entries are zero. M_{S1}^2 and M_{LN}^2 are equivalent to the terminating impedances R_1 and R_N, respectively, in [1].

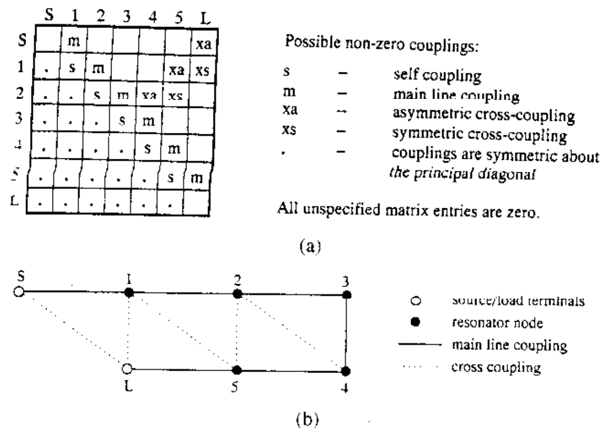

Fig. 4. Folded canonical network coupling matrix form—fifth-degree example. (a) Folded coupling matrix form. "s" and "xa" couplings are zero for symmetric characteristics. (b) Coupling and routing schematic.

Reduction of the $N+2$ Transversal Matrix to the Folded Canonical Form

With N input and output couplings, the transversal topology is clearly impractical to realize for most cases and must be transformed to a more suitable topology if it is to be of practical use. A more convenient form is the folded or "reflex" configuration [9], which may be realized directly or used as the starting point for further transformations to other topologies more suitable for the technology it is intended to use for the construction of the filter.

To reduce the transversal matrix to the folded form, the formal procedure, as described in [1], may be applied, working on the $N+2$ matrix instead of the $N \times N$ coupling matrix. This procedure involves applying a series of similarity transforms ("rotations"), which eliminate unwanted coupling matrix entries alternately right to left along rows and top to bottom down columns, starting with the outermost rows and columns and working inwards toward the center of the matrix, until the only remaining couplings are those that can be realized by filter resonators in a folded structure (Fig. 4)

As with the $N \times N$ matrix, no special action needs to be taken to eliminate unneeded "xa" and "xs" couplings in the cross-diagonals—they will automatically become zero if they are not required to realize the particular filter characteristic under consideration.

Illustrative Example

To illustrate the $N+2$ matrix synthesis procedure, an example is taken of a fully canonical fourth-degree asymmetric filtering function with 22-dB return loss and four TZs, two at $-j3.7431$ and $-j1.8051$, which produce two attenuation lobes of 30 dB each on the lower side of the passband, and two at $+j1.5699$ and $+j6.1910$, producing a lobe of 20 dB on the upper side.

Applying the recursive technique of [1, Sec. II] yields the coefficients for the numerator and denominator polynomials of $S_{11}(s)$ and $S_{21}(s)$

$$S_{21}(s) = \frac{P(s)/\varepsilon}{E(s)} \quad S_{11}(s) = \frac{F(s)/\varepsilon_R}{E(s)}$$

and these are shown in Table I. Being fully canonical, $\varepsilon_R \neq 1$ and may be found from (2). Note that, because $N - n_{\text{fz}} = 0$ and is, therefore, an even number, the coefficients of $P(s)$ have been multiplied by j in Table I.

Now the numerator and denominator polynomials of $y_{21}(s)(=y_{21n}(s)/y_d(s))$ and $y_{22}(s)(=y_{22n}(s)/y_d(s))$ may be constructed using (5). The coefficients of $y_d(s)$, $y_{22n}(s)$, and $y_{21n}(s)$, normalized to the highest degree coefficient of $y_d(s)$, are summarized in Table II.

The next step is to find the residues of $y_{21}(s)$ and $y_{22}(s)$ with partial fraction expansions. Since the numerator of $y_{22}(s)$ ($y_{22n}(s)$) is one less in degree than its denominator $y_d(s)$, finding the associated residues r_{22k} is straightforward. However, the degree of the numerator of $y_{21}(s)$ ($y_{21n}(s)$) is the same as its denominator $y_d(s)$, and the factor K_0 $(=M_{\text{SL}})$ has to be extracted first to reduce $y_{21n}(s)$ in degree by one.

This is easily accomplished by first finding M_{SL} by evaluating $y_{21}(s)$ at $s = j\infty$, i.e., M_{SL} equals the ratio of the highest degree coefficients in the numerator and denominator polynomials of $y_{21}(s)$ [see (7) and (8)] as follows:

$$jM_{\text{SL}} = y_{21}(s)|_{s=j\infty} = \left.\frac{y_{21n}(s)}{y_d(s)}\right|_{s=j\infty} = j0.01509$$

which may be seen is the highest degree coefficient of $y_{21n}(s)$ in Table II. Alternatively, M_{SL} may be derived from (11).

M_{SL} may now be extracted from the numerator of $y_{21}(s)$ [see (9)] as follows:

$$y'_{21n}(s) = y_{21n}(s) - jM_{\text{SL}}y_d(s).$$

At this stage, $y'_{21n}(s)$ will be one degree less than $y_d(s)$ and the residues r_{21k} may be found as normal. The residues, the eigenvalues λ_k [where $j\lambda_k$ are the roots of $y_d(s)$], and the associated eigenvectors T_{1k} and T_{Nk} are listed in Table III.

Note that, for double-terminated lossless networks with equal source and load terminations, r_{22k} will be positive real for a realizable network, and $|r_{21k}| = |r_{22k}|$.

Now knowing the values of the eigenvalues λ_k, the eigenvectors T_{1k} and T_{Nk}, and M_{SL}, the $N+2$ transversal coupling matrix (Fig. 2) may be completed as shown in Fig. 5.

Using the same reduction process as described in [1], but operating upon the $N+2$ matrix, the transversal matrix may be reduced to the folded form with a series of six rotations, annihilating the elements M_{S4}, M_{S3}, M_{S2}, M_{2L}, M_{3L}, and finally M_{13} in order (see Table IV). The resulting folded configuration coupling matrix is shown in Fig. 6(a), and its corresponding coupling and routing schematic is shown in Fig. 6(b).

The analysis of this coupling matrix is shown in Fig. 7. It may be seen that the return loss and rejection characteristics are unchanged from those obtained from the analysis of the original S_{11} and S_{21} polynomials.

III. Transformations of the Coupling Matrix

A microwave filter may be realized directly from the folded coupling matrix, the topology and strengths of its inter-resonator couplings directly corresponding to the nonzero elements of the coupling matrix. However, it is sometimes necessary to apply

TABLE I
4–4 FILTERING FUNCTION—COEFFICIENTS OF $E(s)$, $F(s)$ AND $P(s)$ POLYNOMIALS

s^i i	Coefficients of S_{11} and S_{21} Denominator Polynomial $E(s)$ (e_i)	Coefficients of S_{11} Numerator Polynomial $F(s)$ (f_i)	Coefficients of S_{21} Numerator Polynomial $P(s)$ (p_i)
0	$1.9877 - j0.0025$	0.1580	$j65.6671$
1	$+3.2898 - j0.0489$	$-j0.0009$	$+1.4870$
2	$+3.6063 - j0.0031$	$+1.0615$	$+j26.5826$
3	$+2.2467 - j0.0047$	$-j0.0026$	$+2.2128$
4	$+1.0$	$+1.0$	$+j1.0$
		$\varepsilon_R = 1.000456$	$\varepsilon = 33.140652$

TABLE II
4–4 FILTERING FUNCTION—COEFFICIENTS OF NUMERATOR AND DENOMINATOR POLYNOMIALS OF $y_{21}(s)$ AND $y_{22}(s)$

s^i i	Coefficients of Denominator Polynomial of $y_{22}(s)$ and $y_{21}(s)$ $(y_d(s))$	Coefficients of Numerator Polynomial of $y_{22}(s)$ $(y_{22n}(s))$	Coefficients of Numerator Polynomial of $y_{21}(s)$ $(y_{21n}(s))$
0	1.0730	$-j0.0012$	$j0.9910$
1	$-j0.0249$	$+1.6453$	$+0.0224$
2	$+2.3342$	$-j0.0016$	$+j0.4012$
3	$-j0.0036$	$+1.1236$	$+0.0334$
4	$+1.0$		$+j0.0151$

TABLE III
4–4 FILTERING FUNCTION—RESIDUES, EIGENVALUES, AND EIGENVECTORS

	Eigenvalues	Residues		Eigenvectors	
k	λ_k	r_{22k}	r_{21k}	$T_{Nk} = \sqrt{r_{22k}}$	$T_{1k} = r_{21k}/\sqrt{r_{22k}}$
1	-1.3142	0.1326	0.1326	0.3641	0.3641
2	-0.7831	0.4273	-0.4273	0.6537	-0.6537
3	0.8041	0.4459	0.4459	0.6677	0.6677
4	1.2968	0.1178	-0.1178	0.3433	-0.3433

	S	1	2	3	4	L
S	0	0.3641	−0.6537	0.6677	−0.3433	0.0151
1	0.3641	1.3142	0	0	0	0.3641
2	−0.6537	0	0.7831	0	0	0.6537
3	0.6677	0	0	−0.8041	0	0.6677
4	−0.3433	0	0	0	−1.2968	0.3433
L	0.0151	0.3641	0.6537	0.6677	0.3433	0

Fig. 5. Transversal coupling matrix for 4–4 fully canonical filtering function. The matrix is symmetric about the principal diagonal.

TABLE IV
FOURTH-DEGREE EXAMPLE—PIVOTS AND ANGLES OF THE SIMILARITY TRANSFORM SEQUENCE FOR THE REDUCTION OF THE TRANSVERSAL MATRIX TO THE FOLDED CONFIGURATION. TOTAL NUMBER OF TRANSFORMS $R = \sum_{n=1}^{N-1} n = 6$

Transform Number r	Pivot $[i, j]$	Element to be Annihilated	Fig. 5	$\theta_r = \tan^{-1}(cM_{kl}/M_{mn})$				
				k	l	m	n	c
1	[3, 4]	M_{S4}	in row 'S'	S	4	S	3	−1
2	[2, 3]	M_{S3}	.	S	3	S	2	−1
3	[1, 2]	M_{S2}	.	S	2	S	1	−1
4	[2, 3]	M_{2L}	in column 'L'	2	L	3	L	+1
5	[3, 4]	M_{3L}	.	3	L	4	L	+1
6	[2, 3]	M_{13}	in row 1	1	3	1	2	−1

a further series of rotations to the matrix, to transform it into a form more convenient or more practical to the application in hand, e.g., [10]–[12].

	S	1	2	3	4	L
S	0	1.0600	0	0	0	0.0151
1	1.0600	−0.0023	0.8739	0	−0.3259	0.0315
2	0	0.8739	0.0483	0.8359	0.0342	0
3	0	0	0.8359	−0.0668	0.8723	0
4	0	−0.3259	0.0342	0.8723	0.0171	1.0595
L	0.0151	0.0315	0	0	1.0595	0

(a)

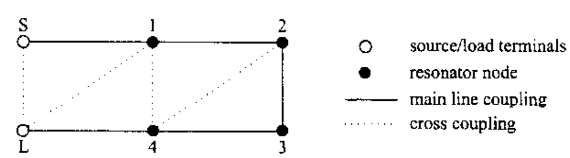

(b)

Fig. 6. Fully canonical synthesis example. Folded coupling matrix for 4–4 filtering function. (a) Coupling matrix. Matrix is symmetric about the principal diagonal. (b) Coupling and routing schematic.

Here, two novel realizations are introduced; parallel-connected two-port networks and the "cul-de-sac" configuration. The first may be derived by grouping residues and forming separate two-port subnetworks, which are then connected in parallel between the source and load terminations. The second is formed by a series of similarity transforms operating upon the folded coupling matrix.

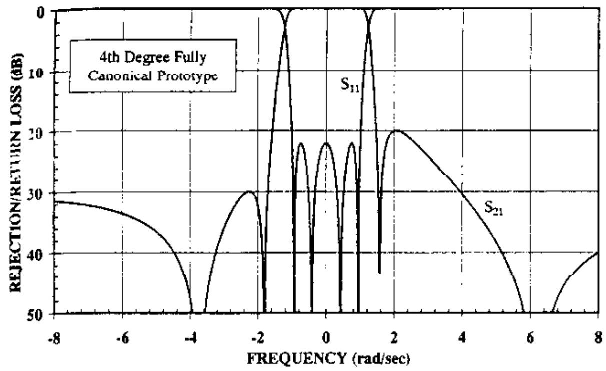

Fig. 7. 4–4 fully canonical synthesis example: analysis of folded coupling matrix. Rejection as $s \to \pm j\infty = 20\log_{10}(\varepsilon) = 30.407$ dB.

A. *Parallel-Connected Two-Port Networks*

Being closely related to short-circuit admittance parameters, the eigenvalues and corresponding residues of the filtering function may be separated into groups and subnetworks constructed from them using the same procedures as described above. The subnetworks may then be connected in parallel between the source and load terminations to recover the original filtering characteristics. The transverse array itself may be regarded as a parallel connection of N single-resonator "groups."

Although the choice of residue groupings is arbitrary, it will be found that difficult-to-realize couplings will be created within the subnetworks, and between the internal nodes of the subnetworks and the source–load terminations if the choice of filtering function and of residue groupings is not restricted. The restrictions are: 1) filtering functions may be fully canonical, but must be symmetric and even degree and 2) residue groups must consist of complementary pairs of residues and eigenvalues, i.e., if the residues with indexes i and j (r_{22i}, r_{21i} and r_{22j}, r_{21j}) constitute a group or are part of a group, then $r_{22i} = r_{22j}$ and $r_{21i} = -r_{21j}$. This implies that only networks double-terminated between equal-value source and load terminations can be synthesized.

If these restrictions are observed, the overall network will consist of a number of two-port networks, the number corresponding to the number of groups that the residues have been divided into, each connected in parallel between the source and load terminals. If the filtering function is fully canonical, the direct source–load coupling M_{SL} will also be present.

Once the residues have been divided into groups, the synthesis of the sub-matrices and their reduction to the folded form follows exactly the same process as for a single network, as described in Section II, working on each subnetwork individually. To illustrate the process, an example is taken of a 23-dB return loss sixth-degree characteristic, with two symmetrically placed TZs at $\pm j1.3958$ producing lobes of 25 dB on either side of the passband, and a pair of real-axis zeros at ± 1.0749 to give group-delay equalization over approximately 50% of the passband. This filter will be synthesized as two subnetworks, one of degree 2 and one of degree 4.

Following the procedure of Section II results in a set of residues and eigenvalues for the characteristic as shown in Table V.

Grouping residues $k = 1$ and 6 yields the folded matrix for the second-degree subnetwork shown in Fig. 8. Now grouping residues $k = 2, 3, 4$, and 5 yields the folded coupling matrix for the fourth-degree subnetwork shown in Fig. 9.

Superimposing the two matrices yields the overall matrix shown in Fig. 10.

The results of analyzing the overall coupling matrix are shown in Fig. 11(a) (rejection/return loss) and Fig. 11(b) (group delay), which show that the 25-dB lobe level and equalized in-band group delay have been preserved.

Other solutions for this topology are available depending on the combinations of residues that are chosen for the subnetworks. However, whatever combination is chosen, at least one of the input/output couplings will be negative. Of course, the number of topology options increases as the degree of the filtering function increases, for example, a tenth-degree filter may be realized as two parallel-connected two-port networks, one fourth degree and one sixth degree, or as three networks, one second degree and two fourth degree, all connected in parallel between the source and load terminations. Also, each subnetwork itself may reconfigured to other two-port topologies with further transformations, if feasible.

If the network is to be synthesized as $N/2$ parallel-coupled pairs (see Fig. 12 for a sixth-degree example), a rather more direct synthesis route exists. Starting with the transversal matrix, it is only necessary to apply a series of rotations to annihilate half the couplings in the top row from positions $M_{S,N}$ back to the midpoint of this row $M_{S,N/2+1}$, i.e., $N/2$ rotations (see Fig. 2). Due to the symmetry of the values in the outer rows and columns of the transversal matrix, the corresponding entries M_{1L} to $M_{N/2,L}$ in the last column will be annihilated simultaneously.

The pivots of the rotations to annihilate these couplings start at position $[1, N]$ and progress toward the center of the matrix until position $[N/2, N/2+1]$. For the sixth-degree example, this is a sequence of $N/2 = 3$ rotations according to Table VI and applied to the transversal matrix:

After the series of rotations, the matrix, as shown in Fig. 12(a), is obtained, which corresponds to the coupling and routing diagram in Fig. 12(b). In every case, at least one of the input/output couplings will be negative. An interesting example of a fourth-degree implementation of this topology realized in dielectric resonator technology is given in [13].

B. *"Cul-de-Sac" Configurations*

The "cul-de-sac" configuration [14] is restricted to double-terminated networks and will realize a maximum of $N-3$ TZs. Otherwise it will accommodate even- or odd-degree symmetric or asymmetric prototypes. It has an important advantage over other configurations in that, whatever the prototype filtering function, there will be only one negative coupling in the entire network and there will be no "diagonal" cross-couplings, which are sometimes awkward to realize in practice. Moreover, its form lends itself to a certain amount of flexibility in the physical layout of its resonators.

A typical "cul-de-sac" configuration is shown in Fig. 13(a) for a tenth-degree prototype with the maximum-allowable seven Tx zeros (in this case, three imaginary-axis and two complex pairs). There is a central "core" of a quartet of resonators in a square

TABLE V
6-2-2 SYMMETRIC FILTERING FUNCTION—RESIDUES, EIGENVALUES, AND EIGENVECTORS

	Eigenvalues	Residues		Eigenvectors	
k	λ_k	r_{22k}	r_{21k}	$T_{Nk} = \sqrt{r_{22k}}$	$T_{1k} = r_{21k}/\sqrt{r_{22k}}$
1	−1.2225	0.0975	−0.0975	0.3122	−0.3122
2	−1.0648	0.2365	0.2365	0.4863	0.4863
3	−0.3719	0.2262	−0.2262	0.4756	−0.4756
4	0.3719	0.2262	0.2262	0.4756	0.4756
5	1.0648	0.2365	−0.2365	0.4863	−0.4863
6	1.2225	0.0975	0.0975	0.3122	0.3122

	S	1	6	L
S	0	0.4415	0	0
1	0.4415	0	1.2225	0
6	0	1.2225	0	0.4415
L	0	0	0.4415	0

(a)

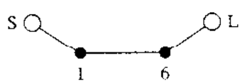

(b)

Fig. 8. Coupling sub-matrix and coupling/routing diagram for residues $k = 1$ and 6. (a) Coupling matrix. (b) Coupling and routing diagram.

	S	2	3	4	5	L
S	0	0.9619	0	0	0	0
2	0.9619	0	0.7182	0	0.3624	0
3	0	0.7182	0	0.3305	0	0
4	0	0	0.3305	0	0.7182	0
5	0	0.3624	0	0.7182	0	−0.9619
L	0	0	0	0	−0.9619	0

(a)

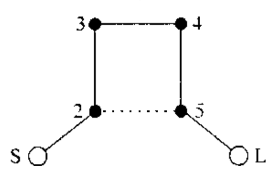

(b)

Fig. 9. Coupling sub-matrix and coupling/routing diagram for residue group $k = 2, 3, 4,$ and 5. (a) Coupling matrix. (b) Coupling and routing diagram.

	S	1	2	3	4	5	6	L
S	0	0.4415	0.9619	0	0	0	0	0
1	0.4415	0	0	0	0	0	1.2225	0
2	0.9619	0	0	0.7182	0	0.3624	0	0
3	0	0	0.7182	0	0.3305	0	0	0
4	0	0	0	0.3305	0	0.7182	0	0
5	0	0	0.3624	0	0.7182	0	0	−0.9619
6	0	1.2225	0	0	0	0	0	0.4415
L	0	0	0	0	0	−0.9619	0.4415	0

(a)

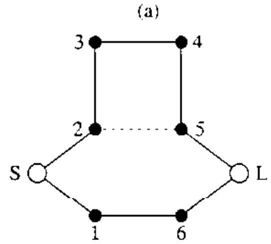

(b)

Fig. 10. Superimposed second- and fourth-degree sub-matrices. (a) Coupling matrix. (b) Coupling and routing diagram.

formation [1, 2, 9, and 10 in Fig. 13(a)], straight-coupled to each other (i.e., no diagonal cross-couplings). One of these couplings

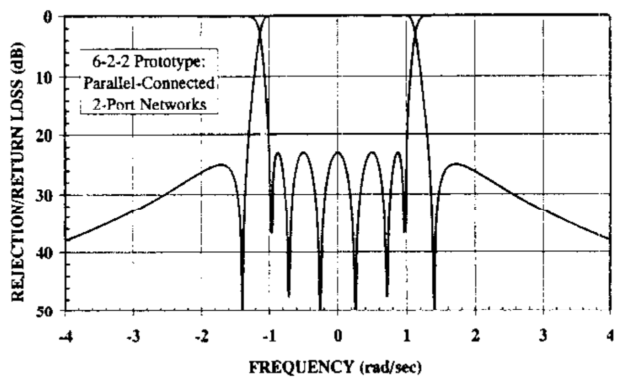

(a)

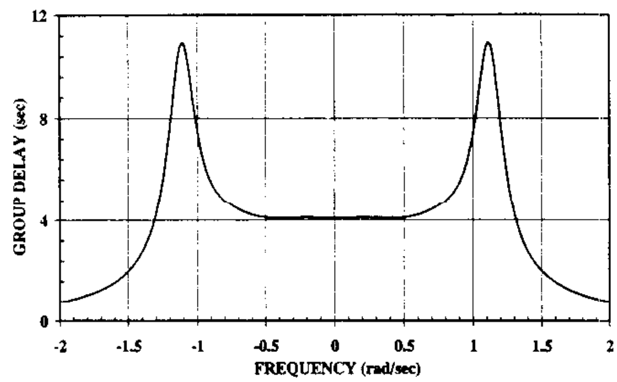

(b)

Fig. 11. Analysis of parallel-connected two-port coupling matrix. (a) Rejection and return loss. (b) Group delay.

	S	1	2	3	4	5	6	L
S	0	0.4415	0.6877	0.6726	0	0	0	0
1	0.4415	0	0	0	0	0	1.2225	0
2	0.6877	0	0	0	0	1.0648	0	0
3	0.6726	0	0	0	0.3720	0	0	0
4	0	0	0	0.3720	0	0	0	0.6726
5	0	0	1.0648	0	0	0	0	−0.6877
6	0	1.2225	0	0	0	0	0	0.4415
L	0	0	0	0	0.6726	−0.6877	0.4415	0

(a)

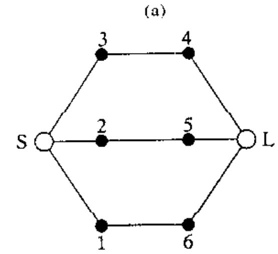

(b)

Fig. 12. Symmetric 6-4 filter example—realized as parallel-coupled pairs. (a) Coupling matrix. (b) Coupling and routing diagram.

TABLE VI
SIXTH-DEGREE EXAMPLE—SIMILARITY TRANSFORM SEQUENCE FOR THE REDUCTION OF THE TRANSVERSAL MATRIX TO THE PARALLEL-COUPLED PAIRS FORMAT

Transform Number r	Pivot $[i, j]$	Elements to be Annihilated	$\theta_r = \tan^{-1}(cM_{kl}/M_{mn})$				
			k	l	m	n	c
1	[1, 6]	M_{S6} (and M_{1L})	S	6	S	1	−1
2	[2, 5]	M_{S5} (and M_{2L})	S	5	S	2	−1
3	[3, 4]	M_{S4} (and M_{3L})	S	4	S	3	−1

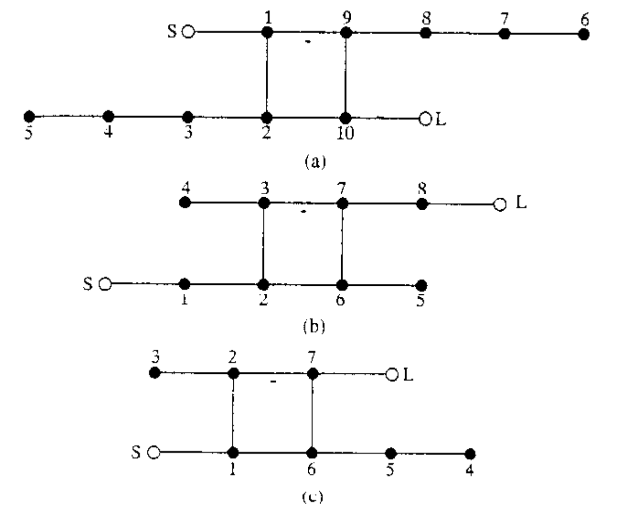

Fig. 13. "Cul-de-sac" network configurations. (a) 10-3-4 network. (b) 8-3 network. (c) 7-1-2 network.

is always negative; the choice of which one is arbitrary. The entry to and exit from the core quartet are from opposite corners of the square [1 and 10, respectively, in Fig. 13(a)].

Some or all of the rest of the resonators are strung out in cascade from the other two corners of the core quartet in equal numbers (even-degree prototypes) or one more than the other (odd-degree prototypes). The last resonator in each of the two chains has no output coupling, hence, the nomenclature "cul-de-sac" for this configuration. Other possible configurations are shown in Fig. 13(b) (eighth degree) and Fig. 13(c) (seventh degree).

C. Synthesis of the "Cul-de-Sac" Network

Fortunately, the synthesis of the "cul-de-sac" network is very simple and is entirely automatic. Starting with the folded coupling matrix, elements are annihilated using a series of regular similarity transforms (for odd-degree filters), and "cross-pivot" transforms (for even-degree filters), beginning with a main line coupling near the center of the matrix, and working outwards along or parallel to the antidiagonal. This gives a maximum of $(N-2)/2$ transforms for even-degree prototypes and $(N-3)/2$ for odd-degree prototypes.

The "cross-pivot" similarity transform for even-degree filters is one where the coordinates of the element to be eliminated are the same as the pivot of the transform, i.e., the element to be annihilated lies on the cross-points of the pivot. The angle for the annihilation of an element at the cross-point is different to that of a regular annihilation and is given by

$$\theta_r = \frac{1}{2}\tan^{-1}\left[\frac{2M_{ij}}{(M_{jj}-M_{ii})}\right] + \frac{k\pi}{2} \qquad (17)$$

TABLE VII
PIVOT COORDINATES FOR THE REDUCTION OF THE $N+2$ FOLDED MATRIX TO THE "CUL-DE-SAC" CONFIGURATION

Degree	Pivot Position $[i, j]$ and Element to be Annihilated — Similarity transform number r; $r = 1, 2, 3, \ldots, R$; $R = (N-2)/2$ (N even) $= (N-3)/2$ (N odd)				Transform Angle
N	$r=1$	2	3	r	θ_r
4	[2,3] M_{23}				eq(17)
5	[2,4] M_{23}				eq(18)
6	[3,4] M_{34}	[2,5] M_{25}			eq(17)
7	[3,5] M_{34}	[2,6] M_{25}			eq(18)
8	[4,5] M_{45}	[3,6] M_{36}	[2,7] M_{27}		eq(17)
9	[4,6] M_{45}	[3,7] M_{36}	[2,8] M_{27}		eq(18)
..	..	..	..	..	..
N (even)	$[i, j]$ $M_{i,j}$ $i = (N+2)/2 - 1$ $j = N/2 + 1$	..	..	$[i, j]$ $M_{i,j}$ $i = (N+2)/2 - r$ $j = N/2 + r$	eq(17)
N (odd)	$[i, j]$ $M_{i,j-1}$ $i = (N+1)/2 - 1$ $j = (N+1)/2 + 1$	..	..	$[i, j]$ $M_{i,j-1}$ $i = (N+1)/2 - r$ $j = (N+1)/2 + r$	eq(18)

	S	1	2	3	4	5	6	7	L
S	0	1.0572	0	0	0	0	0	0	0
1	1.0572	0.0211	0.8884	0	0	0	0	0	0
2	0	0.8884	0.0258	0.6159	0	0	0.0941	0	0
3	0	0	0.6159	0.0193	0.5101	0.1878	0.0700	0	0
4	0	0	0	0.5101	−0.4856	0.4551	0	0	0
5	0	0	0	0.1878	0.4551	−0.0237	0.6119	0	0
6	0	0	0.0941	0.0700	0	0.6119	0.0258	0.8884	0
7	0	0	0	0	0	0	0.8884	0.0211	1.0572
L	0	0	0	0	0	0	0	1.0572	0

(a)

	S	1	2	3	4	5	6	7	L
S	0	1.0572	0	0	0	0	0	0	0
1	1.0572	0.0211	0.6282	0	0	0	0.6282	0	0
2	0	0.6282	−0.0683	0.5798	0	0	0	−0.6282	0
3	0	0	0.5798	−0.1912	0	0	0	0	0
4	0	0	0	0	−0.4856	0.6836	0	0	0
5	0	0	0	0	0.6836	0.1869	0.6499	0	0
6	0	0.6282	0	0	0	0.6499	0.1199	0.6282	0
7	0	0	−0.6282	0	0	0	0.6282	0.0211	1.0572
L	0	0	0	0	0	0	0	1.0572	0

(b)

Fig. 14. "Cul-de-sac" configuration—seventh-degree example. (a) Original folded coupling matrix. (b) After transformation to "cul-de-sac" configuration.

where i, j are the coordinates of the pivot and also of the element to be annihilated, θ_r is the angle of the similarity transform, and k is an arbitrary integer. Note that, for cross-pivot annihilations of M_{ij} ($\neq 0$), where the self-couplings $M_{ii} = M_{jj}$, $\theta_r = \pm\pi/4$. It is also allowable to have $\theta_r = \pm\pi/4$ for when $M_{ij} = 0$, which will give a slightly different configuration alternative. For odd-degree filters, the angle formula takes the more conventional form

$$\theta_r = \tan^{-1}\left(M_{i,j-1}/M_{j-1,j}\right). \qquad (18)$$

Table VII gives the pivot coordinates and angle formula to be used for the sequence of similarity transforms to be applied to the folded coupling matrix for degrees 4–9, and a general formula for the pivot coordinates for any degree ≥ 4.

An example is made of the double-terminated version of the seventh-degree prototype that was used in [1]. This characteristic had 23-dB return loss, a TZ at $+j1.2576$ to give a rejection lobe level of 30 dB on the upper side of the passband, and a complex pair of Tx zeros at $\pm 0.9218 - j0.1546$ to give group-delay equalization over approximately 60% of the passband.

After following the procedure of Section II, the $N+2$ folded matrix shown in Fig. 14(a) is obtained. Applying a series of two similarity transforms at pivots [3, 5] and [2, 6] (Table VII) with angles according to (18) results in the coupling matrix of Fig. 14(b). The corresponding coupling and routing diagram is given in Fig. 13(c).

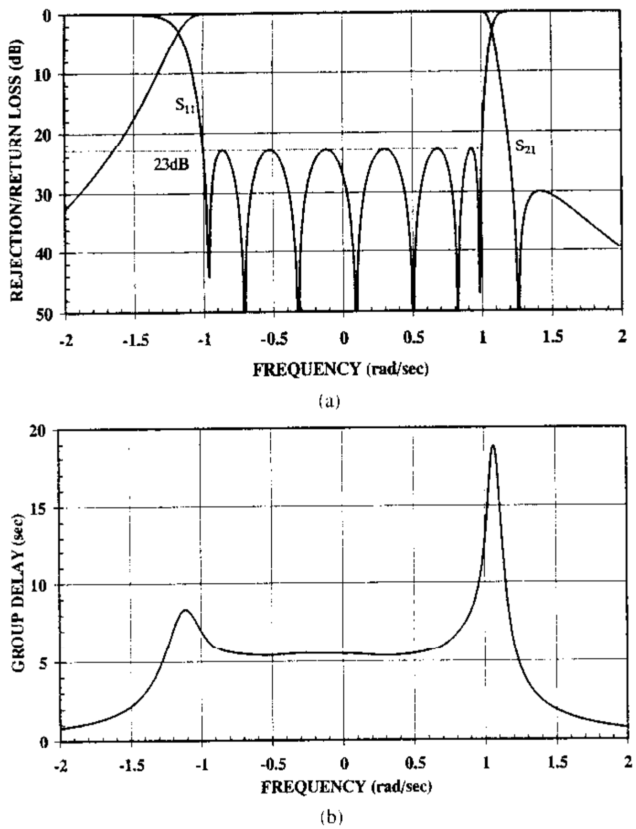

Fig. 15. Seventh-degree "cul-de-sac" synthesis example—analysis of folded coupling matrix. (a) Rejection and return loss. (b) Group delay.

The results of analyzing this coupling matrix are presented in Fig. 15, confirming that the rejection lobe level and group-delay equalization performances have been preserved intact.

As was noted above, all the couplings are positive, except for one in the core quartet. This may be moved to any one of the four couplings for the greatest convenience and implemented as a probe, for example, if the filter is to be realized in coaxial-resonator technology where the other couplings are inductive irises or inductive loops. Also, there are no diagonal couplings even though the original prototype was asymmetric. If it is feasible to implement a diagonal coupling between the input and output of the core quartet, then an extra TZ may be realized, bringing the maximum number realizable by this topology to $N-2$. This coupling in the "cul-de-sac" core will have the same value as in the folded coupling matrix.

IV. Conclusions

In this paper, a simple and general method for the synthesis of the "$N+2$" coupling matrix in the folded cross-coupled array configuration has been presented. The $N+2$ coupling matrix is applicable to symmetric or asymmetric, single- or double-terminated, and even- or odd-degree filtering functions, and will accommodate the fully canonical and multiple-input/output coupling configurations.

The $N+2$ folded coupling matrix may be used directly for the design of a microwave filter if it is convenient to do so, or used as the starting point for the application of a further series of similarity transforms to reconfigure it into a topology more convenient for the technology or production process it is intended to employ. Two examples of such reconfigurations are included in the paper: the parallel-coupled two-port network configuration and the "cul-de-sac" filter configuration. The latter features some important constructional simplifications that should ease the volume production process for high-performance microwave filters for the wireless industry.

Acknowledgment

The author is grateful to Dr. J. D. Rhodes, Filtronics plc. Saltaire, U.K., and Dr. C. Ernst, Lorch Microwave Inc., Salisbury, MD, for useful discussions that aided considerably in the development of the theory presented in this paper.

References

[1] R. J. Cameron, "General coupling matrix synthesis methods for Chebyshev filtering functions," *IEEE Trans. Microwave Theory Tech.*, vol. 47, pp. 433–442, Apr. 1999.
[2] R. E. Collin, *Foundations for Microwave Engineering*. New York: McGraw-Hill, 1966.
[3] I. C. Hunter, J. D. Rhodes, and V. Dassonville, "Dual-mode filters with conductor-loaded dielectric resonators," *IEEE Trans. Microwave Theory Tech.*, vol. 47, pp. 2304–2311, Dec. 1999.
[4] A. E. Atia and A. E. Williams, "New types of bandpass filters for satellite transponders," *COMSAT Tech. Rev.*, vol. 1, pp. 21–43, Fall 1971.
[5] ——, "Narrow-bandpass waveguide filters," *IEEE Trans. Microwave Theory Tech.*, vol. MTT-20, pp. 258–265, Apr. 1972.
[6] A. E. Atia, A. E. Williams, and R. W. Newcomb, "Narrow-band multiple-coupled cavity synthesis," *IEEE Trans. Circuits Syst.*, vol. CAS-21, pp. 649–655, Sept. 1974.
[7] M. H. Chen, "Singly terminated pseudo-elliptic function filter," *COMSAT Tech. Rev.*, vol. 7, pp. 527–541, Fall 1977.
[8] S. Amari, "Direct synthesis of folded symmetric resonator filters with source-load coupling," *IEEE Microwave Wireless Comp. Lett.*, vol. 11, pp. 264–266, June 2001.
[9] J. D. Rhodes, "A low-pass prototype network for microwave linear phase filters," *IEEE Trans. Microwave Theory Tech.*, vol. MTT-18, pp. 290–300, June 1970.
[10] H. C. Bell, "Canonical asymmetric coupled-resonator filters," *IEEE Trans. Microwave Theory Tech.*, vol. MTT-30, pp. 1335–1340, Sept. 1982.
[11] R. J. Cameron and J. D. Rhodes, "Asymmetric realizations for dual-mode bandpass filters," *IEEE Trans. Microwave Theory Tech.*, vol. MTT-29, pp. 51–58, Jan. 1981.
[12] R. J. Cameron, "A novel realization for microwave bandpass filters," *ESA J.*, vol. 3, pp. 281–287, 1979.
[13] V. Pommier, D. Cros, P. Guillon, A. Carlier, and E. Rogeaux, "Transversal filter using whispering gallery quarter-cut resonators," in *IEEE MTT-S Int. Microwave Symp. Dig.*, Boston, MA, 2000, pp. 1779–1782.
[14] A. E. Williams, J. I. Upshur, and M. M. Rahman, "Asymmetric response bandpass filter having resonators with minimum couplings," U.S. Patent 6 337 610, Jan. 8, 2002.

Richard J. Cameron (M'83–SM'94–F'02) was born in Glasgow, U.K., in 1947. He received the B.Sc. degree in telecommunications and electronic engineering from Loughborough University, Loughborough, U.K., in 1969.

In 1969, he joined Marconi Space and Defence Systems, Stanmore, U.K. His activities there included small earth-station design, telecommunication satellite system analysis, and computer-aided RF circuit and component design. In 1975, he joined the European Space Agency's technical establishment (ESTEC, The Netherlands), where he was involved in the research and development of advanced microwave active and passive components and circuits, with applications in telecommunications, scientific, and earth observation spacecraft. Since joining COM DEV International Ltd., Aylesbury, U.K., in 1984, he has been involved in the software and methods for the design of a wide range of high-performance components and subsystems for both space and terrestrial application.

Mr. Cameron is a Fellow of the Institution of Electrical Engineers (IEE), U.K.